



Description of zero field steps on the potential energy surface of a Frenkel-Kontorova model for annular Josephson junction arrays

W. Quapp^{1,a} and J. M. Bofill^{2,b}

¹ Mathematisches Institut, Universität Leipzig, PF 100920, 04009 Leipzig, Germany

² Departament de Química Inorgànica i Orgànica, Secció de Química Orgànica, and Institut de Química Teòrica i Computacional, (IQTCUB), Universitat de Barcelona, Martí i Franquès 1, 08028 Barcelona, Spain

Received 5 March 2021 / Accepted 5 May 2021 / Published online 20 May 2021
© The Author(s) 2021

Abstract. We explain the emergence of zero field steps (ZFS) in a Frenkel-Kontorova (FK) model for a 1D annular chain being a model for an annular Josephson junction array. We demonstrate such steps for a case with a chain of 10 phase differences. We necessarily need the periodic boundary conditions. We propose a mechanism for the jump from M fluxons to $M + 1$ in the chain.

1 Introduction

This paper continues the former two-part series on Shapiro steps [1, 2]. Zero field steps (ZFS) [3] are reported under *dc* bias, thus they are another kind of steps in comparison to Shapiro steps which emerge with an additional frequency of an *ac*-excitation. Josephson junctions (JJs) are electronic superconducting devices. They are reported in the observation of different experiments [4–6]. We concentrate here on the emergence of ZFS in calculations with the Frenkel-Kontorova (FK) model with periodic boundary conditions (PBC) [7]. This paper is devoted to the aim of understanding what happens under a ZFS inside the FK chain, compare the experimental reports in the corresponding Figures 2 in references [8–11], and Figure 4 in reference [12]. To look inside the FK chain we use the potential energy surface (PES) of the chain [13–16] in this work. The PES maps all possible configurations of the chain to their corresponding energy. Of special interest are low-lying pathways, valleys, which connect different stationary structures. The neighborhood of such pathways is the way where the FK chain moves around the ring under an external force, if it was depinned before.

The periodic substrate potential is assumed to be a sinusoidal curve. The annular chain is really of finite length. We search the form of the movement of the FK chain through a site-up potential. Overall, we more deeply treat here the PES for N phase differences (PDs) of the N JJs which are studied in experiments by other workers. We find the PES of JJs rings remained not fully studied until now. The PDs again form a chain.

We search for a global valley through the ‘mountains’ of the N -dimensional PES for a sliding of the chain over the site-up potential. The model changes considerably in comparison to the parts I and II [1, 2]. Additionally, we assume a Josephson phase kink along the array which is called a fluxon [11].

We use the ansatz of an overdamped Langevin equation for a coarse understanding, but the full equation of motion is not further discussed here. Thus, our equations of motion are purely relaxial. Such a treatment is appropriate also for JJs [17]. In contrast to known explanations of ZFS [18, 19] by resonant vibrations, we propose a simpler explanation using the behaviour of the chain under excitation on the PES. The key property of the PES are its nearly vertical walls which cause the steps, without a resonance.

In Sect. 2 we introduce the discrete sine-Gordon (SG) equation and the FK model used in this paper, and we give a preliminary impression of the known case with one fixed fluxon for the case with $N=10$ chain length. In Sect. 3 the case where no fluxon exists is discussed: where all things start with. In main Sect. 4 we calculate and discuss a Langevin equation where we find the ZFS for a *dc*-force (but where also Shapiro steps can emerge if one applies an *ac*-force [1]). In Sect. 4.2 we propose a mechanism for the transition from $M = 0$ fluxons to $M = 1$, and in Sect. 4.4 we propose another mechanism for the transition from $M = 1$ fluxons to $M = 2$ being probably the general jump for a step from M to $M + 1$. In Sect. 5 we additionally report the structures of stationary states of the chain for $M > 2$. Finally the last sections are devoted to some discussions and a conclusion.

^ae-mail: quapp@math.uni-leipzig.de (corresponding author)

^be-mail: jmbofill@ub.edu

2 The sine-Gordon (SG) equation and the FK model

One single JJ has already a rich set of properties which can be described by a 1D SG in dimensionless form

$$\ddot{\phi} + \eta \dot{\phi} = -\sin(\phi) + F \tag{1}$$

where $\phi(t)$ describes a high frequent phase difference (PD) between the two superconducting layers of the JJ [6,20], η is a damping factor, and F is the current through the JJ.

In the more general case, the vector $\Phi = (\phi_1, \dots, \phi_N)$ represents the value of N superconducting PDs on the corresponding i th junctions [18] of an annular chain. Now generally it does not hold that $\phi_i < \phi_{i+1}$ for $1 \leq i \leq N$, in contrast to parts I and II [1,2]. The chain has the equilibrium distance, $a_o = 0$, and the ϕ_i can change their order. An array of parallel JJs is described by a system of discrete SG equations [6,18]

$$\ddot{\phi}_i + \eta \dot{\phi}_i = -\sin(\phi_i) + k(\phi_{i+1} + \phi_{i-1} - 2\phi_i) + F \tag{2}$$

where the index i runs over certain integers, for a first ansatz. The periodicity $a_s = 2\pi$ is used throughout for the site-up potential of the JJs, and k is the ‘spring force constant’ between the PDs. F is an external force which is equally applied to all ϕ_i [18]. The number of JJs in the ring is N . The ‘geometry’ of the JJs is fixed, also the ‘distances’ between the JJs. However, here a property of the JJs counts, the superconducting phase difference. It can be zero for all JJs, but usually it changes. The PDs, ϕ_i , are the ‘variables’ of the FK model. They are the former ‘particles’. The handling of the periodicity of a ring of JJs needs deeper attention. Traditionally periodic boundary conditions (PBC) [11,17,21] were used

$$\phi_{N+i} = \phi_i + 2\pi M, \text{ for all } i, \tag{3}$$

with an integer M . At first glance the PBC are ‘disturbing’ because for $M > 0$ the PD with number i and the PD with number $i + N$ are not equal though they belong to the same JJ. The contradiction is solved by the action of the PDs on the site-up potential, $\sin(\phi_i)$ which is periodic with 2π . To give the same value for i and $i + N$, the number M in the PBC must be an integer. M counts the ‘fluxons’ trapped in the chain which emerge under the cooling of the experiment with a magnetic field [9]. In Sects. 4.2 and 4.4 below we try to explain how a jump from M to $M + 1$ can happen.

The first action of the PBC with a given N is that the formally infinite system (2) is reduced to N equations [22]. Thus the PBC act like a modulo specification. On the other hand, the variable M in the PBC is assigned to the number of ‘fluxons’, thus kinks which are trapped in the chain [21]. One or more fluxons enforce a difference between the PDs. The frustration is named by $\delta = M/N$, and the average distance between the PDs becomes $\tilde{a}_0 \approx 2\pi\delta$. Note that this is not the

real distance between all the PDs, like it is claimed [23,24], compare Fig. 1. The average length of the chain is $|\Phi| \approx 2\pi M(N - 1)/N$. In Sect. 5 we discuss that it has to hold $\delta \leq 1/2$ in a JJs ring.

We treat the harmonic spring potential which is the background of the discrete SG of Eq. (2) [17,25,26], and an additional ring potential

$$S_{\text{ring}}(\Phi) = \frac{k}{2} \sum_{i=1}^{N-1} (\phi_{i+1} - \phi_i)^2 + \tag{4}$$

$$\frac{k}{2} (\phi_1 - \phi_N + 2\pi M)^2. \tag{5}$$

The usual distance in the chain, a_0 , of the other FK models of parts I and II [1,2], is put to zero here. The first sum (4) is the inductive energy of the chain [26]. The last summand (5) is the contribution to the PBC. The relation of the periodicity of the sine function in (2), 2π , and the frustration may strongly affect the spatial structure of the system. The PES for the variable changes of the ϕ_i is the Frenkel-Kontorova model

$$V(\Phi) = P(\Phi) + S_{\text{ring}}(\Phi) \tag{6}$$

where the site-up P is the potential

$$P(\Phi) = \sum_{i=1}^N (1 - \cos(2\pi \phi_i/a_s)). \tag{7}$$

(Note $k = 1$ and $a_s = 2\pi$ is used in the paper.) The ring potential (5) enforces a chain of a length of $\approx 2\pi M$. The number N of JJs in the chain is packed into this interval.

In the JJ-ring model, the ring condition of the periodic boundaries comes to its intrinsic right. The ring structure of the JJs enforces the 2π -modulo relation of all the ϕ_i . It organises, on the other hand, that at the boundaries no disturbing reflections emerge [3,8], and so that the array prevents anti-fluxons [18].

We use a short chain with $N = 10$ PDs and $M = 1$. The parameters could be achieved in a typical experiment. In Fig. 1 we represent two known stationary points of the chain, a minimum and a saddle point of index one (SP₁). Their energies are 7.868 and 7.894 units, correspondingly. The ring condition really makes a chain in the box with the length 2π . The chain itself is stretched over the full box and thus forms a kink, in comparison to a solution with zero distances corresponding to $a_0 = 0$.

Note that the ‘centre of mass’ of the chain [17,18] is probably not a good measure for the annular chain, because the beginning and the end of the numbering are arbitrary. Formally one can describe the movement of the chain along the Φ -axis. However, then the ϕ_j are not periodic functions, like the PBC enforces it, by the relation modulo $2\pi M$. To Fig. 1 belong still nine other equivalent minimums and SP structures with a further moved numbering: compare Fig. 2. After 5 steps

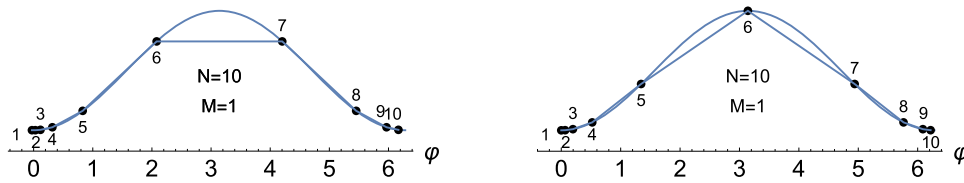


Fig. 1 Equilibrium structures (minimum left and SP_1 right [17,20]) of the FK chain with $N = 10$ PDs under the ring condition (5) with $M = 1$. The bullets are artificially lifted on the potential to guide the eye. Because we use $a_0 = 0$ in the model potential (4), the PDs can form ‘nearly together lying clouds’ in the minimums of the cosine function

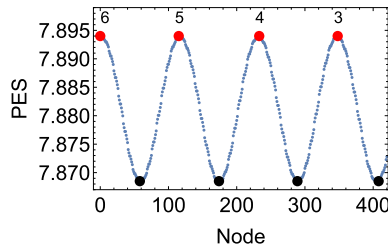


Fig. 2 Energy profile over a piece of the MEP through minimums (black) and SP_1 (red) calculated by a Newton trajectory (NT) [2] to a unitary direction (1, . . . , 1). On the theory of NTs see part II. The numbers over the SPs depict the consecutive ϕ_k which cross the SP. Note the very low energy difference of the two stationary points. Thus, the pathway is nearly flat, and the critical current is very low

on the minimum energy path (MEP), the PD ϕ_1 crosses the SP_1 but all other ϕ_j are collected in the next well around 2π . For both structures of Fig. 1, minimum and SP_1 , the bottom of the well contains 6 to 8 PDs, but two PDs are sitting on top, for the minimum, or only one PD is placed there, for the SP_1 . To describe a movement of a fluxon, it is better to say which single PD currently crosses the top of the site-up potential. Having in mind the PBC (3) we can say that the ‘centre of mass’ of the chain is on the opposite side of the active ϕ_k where the set of the other ϕ_j jostles.

The energy profile of the global valley line of the PES is shown in Fig. 2. We calculated an NT to the unit direction. The nodes depict points on the step length axis. We use a predictor step of 0.0125. Of course, one can also reproduce the MEP by consecutive steepest descends from the SPs [17]. Every top is an SP_1 to the consecutive ϕ_j . Corresponding numbers j are put over the SPs beginning with the $j = 6$ of Fig. 1. Though the energy difference between the SP_1 and the minimums is very low, it is not zero. This is important in comparison to the continuum SG model [17]. But the nearly zero energy difference on the MEP causes in the experiments that the depinning current nearly vanishes, and that the voltage starts to increase as soon as current is injected [12].

An imagination of a movement of the chain along the MEP of Fig. 2 sees the consecutive ϕ_k climbing over the SP_1 -structure, the right one in Fig. 1. But every such passage is followed by a descent of the structure to the next, consecutive minimum, where ϕ_{k-1} and ϕ_k are the two PDs next to the top. The movement

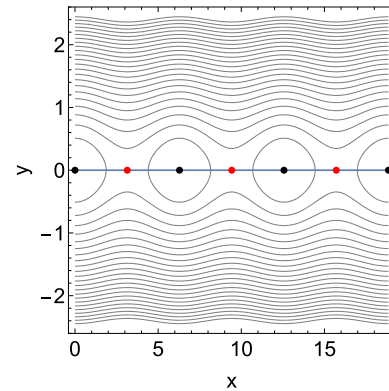


Fig. 3 Schematic 2D contour line projection of the PES of the 10-chain. The central $y = 0$ -line is the model of the MEP of Figs. 1 and 2. The minimums are black bullets, but the SP_1 are red bullets. So to say, the x -coordinate is the direction along with the MEP but the y -coordinate collects all the $(N - 1)$ directions orthogonal to the MEP. The parameter M can run from 1 to 9, compare Sects. 4.3 and 5

looks like a wave. The form of the passage is always the same, however, there is no fixed quasiparticle. The chain changes continuously its shape. The distances around the ‘climbing’ ϕ_k are large, where the distances between the PDs in the wells are short or zero. By the PBC (3) we have a periodicity. After $N = 10$ steps the numbering of the climbing ϕ_k repeats. But we do not have an invariant chain with respect to discrete translations from ϕ_k to ϕ_{k-1} [27] what many workers claim.

In contrast to the model of Part II of this series [2] where the valley through the PES mountains has some ‘floors’ with SPs with an increasing index, (in case of $N=8$ with two central SPs of index 4) and complicated relations between the floors, here we find a very simple PES with only one ‘floor’ being at the same time the ground valley. The floor line is the profile over the MEP over the minimums and SPs of index one of Fig. 1. In Fig. 3 we suggest a 2D schematic projection of the full PES. Of course, this is an oversimplification. One should also note that the straight line of the MEP here is curvilinear in the real chain because every minimum, and every SP_1 are located in other dimensions of the 10D configurations space. Note, the chain continuously changes its internal distances between the ϕ_i if it moves along the MEP of Fig. 2. The most ‘single’ ϕ_j is the PD of number j which currently goes over the top of the cosine function at the SP_1 .

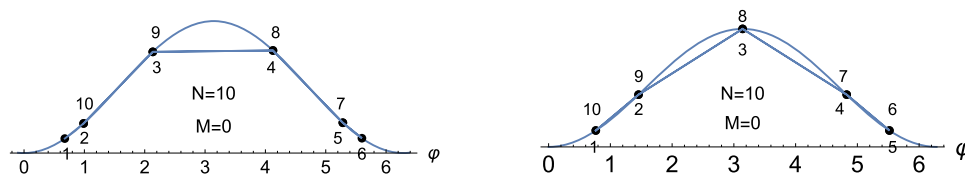


Fig. 4 Extended SP_1 (left) and SP_2 (right) for $M = 0$. The left numbering of the PDs goes from 1 to 6 with increasing value, but then back. So that $\phi_{6+k} = \phi_{6-k}$, $k = 1, \dots, 4$ where for the right hand case it goes up to $i = 5$ and then symmetrically back. Besides the foldings, the structures look like the minimum and the SP_1 of the $M = 1$ -case in Fig. 1

The move of the fluxon along the MEP is a stringent proof against the assumption [17, 27] that the chain is rigid and moves as a rigid quasiparticle. What is quasi ‘fixed’ is the continuously alternating change of the minimum- and the SP_1 -structure where the single PDs run through their numbering but the chain goes on in Φ -direction.

The on-site potential will modulate the chain if an external further force is applied. We use a linear force by application of a current to the JJ-ring [21, 28–31]. It makes an effective PES

$$V_{\text{eff}}(\Phi) = V(\Phi) - F (l_1, \dots, l_N)^T \cdot \Phi. \quad (8)$$

We mainly use the standard N -dimensional normalised force vector $(l_1, \dots, l_N)^T = 1/\sqrt{N} (1, \dots, 1)^T$. F is the factor for the amount of the external force. In this paper we sometimes suppress the factor $1/\sqrt{N}$ in the formulae for simplicity. The gradient of $V_{\text{eff}}(\Phi)$ is used for the construction of the equation of motion (2).

The external term is named dc driving [32, 33] (for direct current) if F is fixed. If the amount of the force alternates in time then one names it ac driving [34] (for alternate current). The force tilts the former on-site potential for PD ϕ_i with the incline $F l_i$, $i = 1, \dots, N$. The extremal points of the effective PES, V_{eff} , minimums and SPs, move if F increases. A corresponding curve is described by a Newton trajectory (NT) [35–39].

The spring constant, k , in Eqs. (2) and (4) is often represented as a ‘discretisation’ parameter $k = 1/a^2$. This imagination is coming from the connection to the continuum SG [40]. If we take the limit $a \rightarrow 0$, $ia \rightarrow x$ and $\phi_i \rightarrow \phi(ia)$, we get for $1/a^2 \sum_{i=1}^N (\phi_{i+1} + \phi_{i-1} - 2\phi_i)$ the second derivative, ϕ_{xx} , to a length coordinate, x , for corresponding decreasing distances between the ϕ_i . Here we understand the parameter, k , as the spring constant in the FK model.

3 Preliminary treatment of the PES of an FK chain with $M = 0$

The ring condition secures, in the case $M = 0$, that we first get a rigid vector, Φ . If we move it by a sufficiently strong extended unitary force then it will overcome the top of the cosine function of the site-up potential. The ground state of the chain is the sitting of every PD in one and the same well of the cosine function. The lowest

eigenvalue of the Hesse matrix of the PES there is 1, and the corresponding eigenvector of the first normal mode is pure translational vibration [30]. This movement leaves the chain unchanged, it only vibrates ‘collectively’ in this one well.

We can excite the vector of PDs over the critical force, $F_c = \sqrt{10}$, for the equal bias on all PDs. Then we get a sliding behaviour. It moves like a lump of narrow points over the site-up potential. The lump whirls over the SP of the cosine potential [41]. The minimum of the PES is all in all $\phi_i = 0$ with energy zero, but an SP is for all $\phi_i = \pi$ with energy 20 units. Thus the energy difference for this path is much larger than in the case $M = 1$, compare Fig. 2. However, the SP has index three.

So, there is a lower SP anywhere. We get it by a PDs chain which first extends along the axis, but then folds back, so that the last ϕ_N comes back to the beginning to fulfil the ring condition, $M = 0$. Its energy is 15.256 units, see left panel of Fig. 4 for an illustration. A steepest descent on the left-hand side goes to the minimum $\phi_i = 0$ for all i , but on the right-hand side it goes to the minimum $\phi_i = 2\pi$ for all i . In Ref. [7] such a structure is named fluxon-antifluxon pair, though the name is not explicitly explained there. We will question such a description. What is here the anti-structure? The concept kink-antikink means stretching or compression of the structure of a chain. For $M = 0$ and a lumped set of PDs, there a further compression cannot take place. Only the kink-concept of a stretching can be applied. We think that the description by the words ‘folded chain’ is better. Maybe one could also say ‘folded kink’. But nevertheless, the report of such states in Ref. [7] leads us to the search, and finally to the detection of this state.

The exorbitant higher energy difference of the SP_1 to the minimum in this case, $M = 0$, in comparison to the ‘flat’ MEP of the $M = 1$ case, see Fig. 2, makes a qualitative different behaviour. Without reference to a possible case of $M = 0$, this is named ‘parasite’ pinning [11]. Compare Sect. 4.1 below where we further treat this case.

Closely nearby in energy is also the next index SP, the SP_2 , with 15.294 units of energy, see the right-hand side of Fig. 4. We could not find any further SPs on the PES for $M = 0$. The reported further structures in Ref. [7], in the case $M = 0$, have to be of dynamical character. It would be an interesting task to illustrate their localisation on the PES between the three SPs.

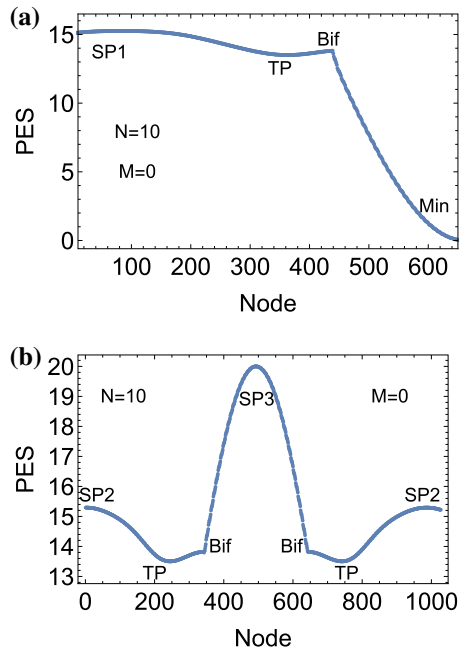


Fig. 5 Energy profiles of NTs from SP₁ (a) and from SP₂ (b) for $M = 0$. The search direction is the unitary one. Both NTs bifurcate at a VRI point

Profiles over NTs starting at both SPs of index one and two are shown in Fig. 5. Both curves bifurcate at a valley-ridge inflection point (VRI), and unite after this with the global minimum or the higher SP₃. The VRI point is the structure with all $\phi_i = 1.97$ for $i = 1, \dots, N$, thus again a lump of points. It is on the fully symmetric pathway from minimum to SP₃ with the rigid ‘chain’. One could speculate that the symmetry breakdown at the VRI point opens a lower pathway for a moving chain than the fully symmetric path over the SP₃. See Sect. 4.1 below for the description of such a path.

The two SPs of index one and two are connected by an annular ridge of the PES, quite as the MEP of Fig. 2. We found an artificial NT to the direction of the first positive eigenvalue of the SP₁ which connects in a continuous way the series of the two stationary points by a consecutive ‘rotation’ of the PDs where the chain stays on the place. The search direction of the NT is $\mathbf{l}_{rot} = (0, 0.19, 0.46, 0.46, 0.19, 0, -0.19, -0.46, -0.46, -0.19)$. The profile of the NT is shown in Fig. 6a. In Fig. 6b the final structure of the chain at the end of the NT is represented which nicely shows the rotation of the PDs where the vector Φ stays all in all on its place.

4 The overdamped Langevin equation

The components of the gradient of the effective PES are

$$g_{eff\ i} = k(\phi_{i+1} + \phi_{i-1} - 2\phi_i) - v \sin(\phi_i) + F l_i \quad (9)$$

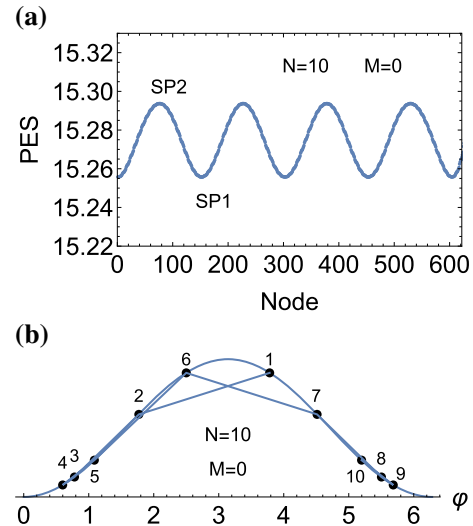


Fig. 6 a Energy profile over a piece of an NT through consecutive SP₁ and SP₂, for $M = 0$. The search direction of the NT is the first positive eigenvector of SP₁. The NT balances on a ridge. b A stroboscopic structure at the end of the NT: the PDs are ‘rotated’ where the chain stays on the place. Compare the order in Fig. 4

for $i = 1, \dots, N$. For $i = 0$ and $i = N + 1$ here emerge additional particles which are connected over the PBC [25]. They form the ring of this FK model, see Sect. 2. If we put the gradient to zero, we get the ansatz of the NT theory [13]. In contrast, one can put the gradient into a steepest descent equation, and one can name it the overdamped Langevin equation [43, 44]

$$\eta \dot{\Phi} = -\mathbf{g}_{eff}(\Phi). \quad (10)$$

For JJs systems, the full Eq. (2) is usually the correct description. However, if one shunts each JJ by a resistance then one can get a correct description by the overdamped dynamics [17]. Numerically we approximate solutions of Eq. (10) with t -steps of length 0.001, 0.005, or 0.01. In corresponding representations we depict the time axis by ‘node’.

If one chooses $F > F_c$, the critical force, in the Langevin equation then a positive amount emerges for the velocity of a change of the chain. By the stronger tilting of the force, F than F_c , the chain will be depinned and slides ‘downhill’ the effective PES. However, by the PBC we get a rotation of the chain around the annular JJs array.

4.1 Movement of an FK chain for $M = 0$

We remember that the ground state of the chain is the lump of PDs in one and the same well of the cosine function. The movement under the equal excitation $F/\sqrt{10}(1, \dots, 1)$ leaves the chain unchanged. We have to report that this pathway is quite stable. If we start in the unsymmetrical SP₁ then a Langevin solution first correctly relaxes to the region of the global minimum

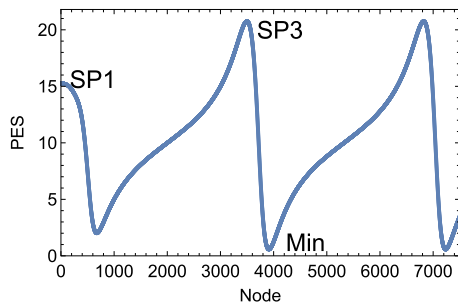


Fig. 7 Energy profile over a Langevin solution on the PES only (without representation of the tilting, compare parts I and II [1,2]) starting at SP₁, for $M = 0$. The excitation direction is the unique case, $(1,1,\dots,1)$, and the amount, $F_{dc} = 3.5$ is a bit over the critical force, $F_c = \sqrt{10} = 3.16$. After settling in the first cycle, the solution alternately crosses the regions of the minimum and of the SP₃

and then goes the way over the fully symmetric SP₃, see Fig. 7 for a corresponding energy profile. Note that we use a reduced representation, without the part of the external bias, the PES only, compare parts I and II [1,2].

If one is on the PES for $M = 0$ then the ‘collective’ unified movement of the chain as a lump, over an SP of index 3, is not the direction to a lower energy path through the PES mountains. This should go over the region of the SP₁. We found such pathways for other external excitation directions. One may imagine that in the array of JJs not all currents through every single JJ are equal. Then the vector of the force, \mathbf{l} , may be not the vector of equal entries. Or one can imagine a disorder by thermal noise. Here we use $\mathbf{l} = (0.3, 0.39, 0.48, 0.23, 0.1, 0.07, 0.1, 0.23, 0.48, 0.39)$. It is the direction of the gradient in the barrier breakdown point (BBP) [2] of the steepest descent from the SP₁ downhill. The result of a Langevin solution is shown in Fig. 8. The amount of the external force is $F_{dc}=3.2$. We still illustrate the 4 turning points (TP) of the solution of Fig. 8, in Fig. 9. M1 is near an SP₂ and one can observe that ϕ_3 and ϕ_9 climb over the top of the site-up potential. The point m1 is nearer to an SP₁ and the pairs $\phi_4 - \phi_3$ and $\phi_8 - \phi_9$ are on top. For M3 already the ϕ_4 and ϕ_8 are over the top, it is again nearer to the SP₂ structure.

4.2 Middleton’s rule, jump of $M = 0$ to $M = 1$

In contrast to the NT in Sect. 3, for $M = 0$ does not exist a stable Langevin solution staying only on the ridge between the two SPs of index one and two, as one could speculate with the result of the NT. In Fig. 10 we show the solution with the start at SP₂ to the not-unique eigenvector of the former NT and an $F_{dc} = 0.1$. It comes back, really once times, on the PES only (compare parts I and II [1,2]) to the region of the SP₂, but then it descends after a longer sliding to the minimum where it is fixed caused by the small F_{dc} far below the critical force. The first loop is, so to say, still a settling phase.

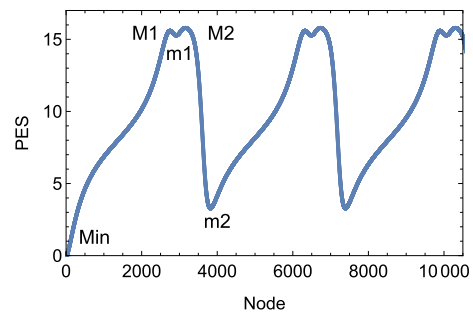


Fig. 8 Energy profile of a dc-driven Langevin solution on the PES only for $M = 0$ and for $F_{dc} = 3.2$. The excitation direction is a gradient vector, see text. We find a stable vibration after an initial settling

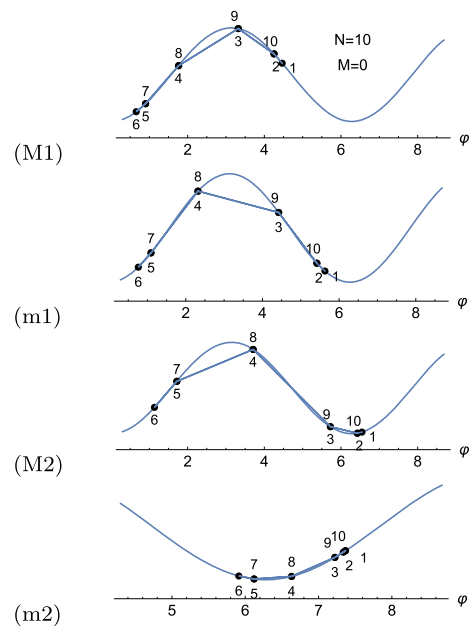


Fig. 9 Structures of the TPs for the movement of the chain in Fig. 8 for $N = 10, M = 0$. The pattern repeats for every next cycle of the sliding

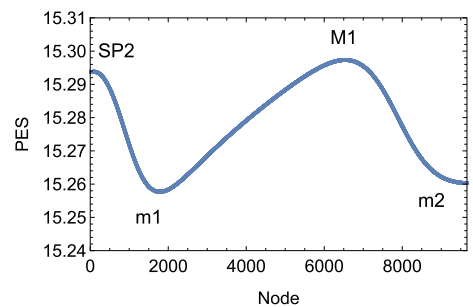


Fig. 10 Energy profile (PES only) over a Langevin solution starting at SP₂, for $M = 0$. The bias direction is the first positive eigenvector of SP₁, \mathbf{l}_{rot} of Fig. 6. The excitation amount is $F_{dc} = 0.1$, but the step length of t -steps is 0.01. After step 15,000 it descends to the global minimum (not shown). M1, m1, and m2 are maximal and minimal TPs

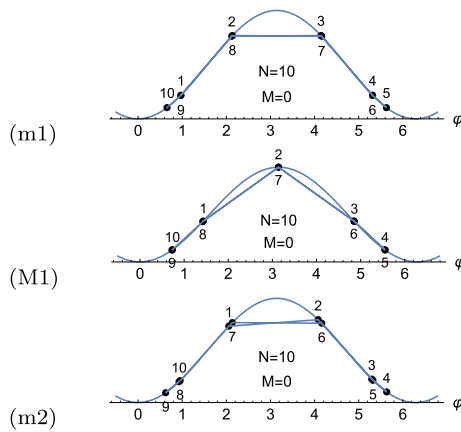


Fig. 11 Structures of the TPs of the Langevin solution of Fig. 10 for $N = 10, M = 0$. Note the rotation of the PDs from (m1) to (m2), or from SP_2 (Fig. 4, right panel) to (M1)

The rotation of the PDs in the folded kink, on the profile of the cosine function reported in Fig. 11, contradicts the Middleton’s no-passing rule [45] because the rotation destroys the given order of the chain at an initial structure. One reason may be the not-unique force vector with alternating signs. Compare, however, another case in Sect. 4.4 below.

On the other hand, if one images a rotation by 3 places of all PDs, starting with the SP_1 of Fig. 4 left, or still better a rotation by 8 places, then one gets the PDs ‘sorted’ in the kind that on one side of the cosine function one half of numbers is collected, 1–5, and on the other side the numbers 6–10 are collected.

Gedankenexperiment

Now one can imagine a cut of the ring potential (5) with the $M = 0$ parameter. Thus we solve the ‘bond’ between $\phi_1 = \phi_{11}$ and ϕ_{10} . The structure of the folded chain will relax to a minimum where one half of the PDs collects at the left hand well, but the other half collects at the right hand well. It can relax to a minimum of the chain of the case with PBC $M = 1$. The minimum structure itself (see Fig. 1) does not make a contribution to the PBC.

Of course, the special ring condition (5) with ϕ_1 and ϕ_N only is contributed to the numbering; so, every SP_1 -‘bond’ of the folded chain can tear. In Fig. 4 left it concerns the bond 3-4 or 8-9.

The ring condition itself is necessary to guarantee the ring structure of our problem. However, which M one should put? This is arbitrary. So, under the excitation of the last subsections, one can guess that it is possible that the system jumps to the next M . The given M is conserved by our formula (5) but probably not in the real chain. There only any M must rule the ring character. Reference [12] describes that M is ... “determined by the initial conditions, but remains constant throughout the subsequent evolution of the system ...” The initial conditions are put by an orthogonal magnetic field of

M flux quanta, $M\Phi_0$ [9,46] which is applied before the experiment. See a further discussion in Sect. 5.

So to say, JJ arrays in ring form have the dimension $(N + 1)$ where N dimensions describe the N JJs but the $(N + 1)$ st dimension describes the number of fluxons. Of course, the last coordinate, M , can only assume discrete integer values, but it can jump.

Up to now, we cannot combine the optimisation of the N usual dimensions with the extra M . But we can change the M in our formula by hand. Compare a similar remark in Ref. [10], as well as: “while the fabrication of annular junctions is rather easy, trapping of fluxons in them remains a difficult art” [42]. In experiments, it is reported that JJs arrays really jump between the M -‘coordinate’ [10,20]. Thus nature finds these ‘worm-holes’ between the different M -worlds. See Sect. 4.4 below for a further propose how it could work.

4.3 The movement of an FK chain for $M = 1$

Here we have again a box of 10 elements of the JJs ring. However, now by $M = 1$ we allow a ‘fluxon’ of the PDs, to emerge in the ring [7,9,20]. It acts like an enforcement of an SP_1 respective an intermediate minimum for the chain; it is shifted to the first floor of the PES of a chain with $N = 10$ particles and free boundaries [15]. However, this first floor now has no end. It is periodic along the JJs ring.

In Fig. 12 we show calculations of a ‘sliding chain’, a solution of the Langevin Eq. (10) with a unique force, which quickly finds the region over the MEP and then there goes on up to infinity. Note that the pathway of the MEP is (for $k = 1$) quasi flat.

Note that the profiles still follow the pattern of the MEP between the minimum and the SP_1 of the chain in Fig. 2, but on an increasing level of energy. The external force acts uniformly on all ϕ_i , not only on the one ϕ_k which actually overcomes the top of the site-up potential. The decay direction for the PD ϕ_6 (see Fig. 1) being on the top of the sine potential is the eigenvector (0.02, 0.03, 0.06, 0.16, 0.41, 0.78, 0.41, 0.16, 0.06, 0.03). This is not the unique excitation direction of the JJs ring. So, we have an unnecessary force effort to all parts of the chain, where one only needs the force f_k to act on the one ϕ_k . This accumulates a great amount of the external force to move the one ϕ_k further, and then the next ϕ_{k+1} , and so on. The increase of the energy of the profile line of the different cases with increasing F_{dc} demonstrates the effect.

In panel Fig. 12a we find, after a short settling, that the flow oscillates by a fixed, but low frequency. The profile repeats the MEP of Fig. 2, however, on a higher energy level. The minima and maxima of the profile are turning points (TPs) but not stationary points of the PES.

To panel (b): after $\approx 10,000$ t-steps (nodes) the chain slides ‘down’ the tilted effective PES by a stable flow, and with a much higher frequency than in case (a). However, the amount of the vibration decreases. The

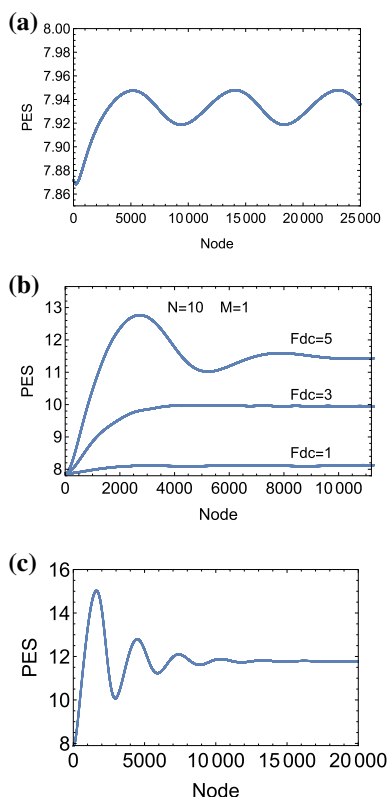


Fig. 12 Energy profile of dc-driven Langevin solutions on the PES only (without representation of the tilting, compare parts I and II [1, 2]) for $N = 10, M = 1$ and direction $(1, \dots, 1)$. **a** For $F_{dc} = 0.15$, somewhat over the critical force $F_c = 0.02542$, with the start in a minimum, **b** the profiles for $F_{dc} = 1, 3$, and 5 , **c** for $F_{dc} = 7.5$. We find a stable small vibration in cases **a** and **b** after an initial settling. In case **c** the curve flattens out

projected profile on the original PES is much higher than the MEP.

To (c): a giant settling after the large F_{dc} causes a ‘collective’ push of the chain of PDs, thus of all ϕ_i , to an inversion of the former positions. In low energy positions most ϕ_i are in the well of the cosine function. However, in high energy positions they are on the top of the cosine function. After $\approx 15,000 t$ -steps the vibration flattens out and ‘stays’ without any vibration at 11.784 units. One could imagine that the frequency increases to ‘infinity’, in comparison to case (b), but the amount of the vibration decreases to zero. Thus, the external force drives the chain along a level line of the PES. The small difference between the minimum and the SP_1 is totally flattened out.

In Fig. 13 is shown a moment structure to case (c). The diverse PDs nearly have equal distances, compare reference [12]. However, the distances are still not totally equal, here. They are at the structure of Fig. 13 $\Delta\phi = (0.56, 0.55, 0.57, 0.62, 0.67, 0.71, 0.71, 0.68, 0.63)$. Note that we have shortened the representation by the transformation of the chain to the initial interval by the PBC modulo relation with 2π .

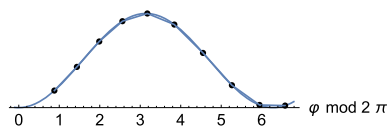


Fig. 13 Stroboscopic picture of the structure of the chain in case of Fig. 12c for $F_{dc} = 7.5$ at the end of the calculated time. The chain comes already near to an equidistance between the PDs, the blue bullet in Fig. 14

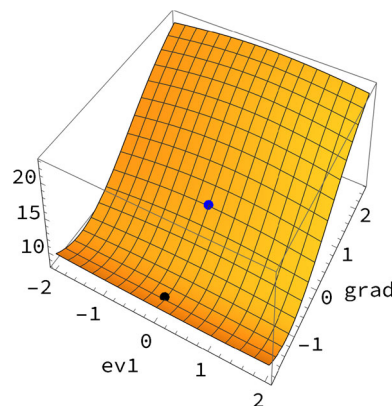


Fig. 14 2D projected picture of the PES of the 10-chain at the equidistant structure of the chain (the fat blue bullet at coordinate $(0, 0, V)$). This point is probably a VRI point. The two directions are the gradient there, and the one negative eigenvector of the Hessian. By the black bullet we depict a minimum

The transition from a ‘stable’ wave as in Fig. 12b to a flat curve as in panel 12c goes on quasi continuously for the Langevin solution. For the continuum SG equation, however, it has a singularity, see Fig. 2 of reference [12].

How far can the pathway be moved uphill? Or in other words: is there an end for F_{dc} ? Like the observed Zero-field steps (ZFS) would mean [8–11]. A similar figure like 12c we get for $F_{dc}=10$, where the level of the flat final line is at an even higher energy of 11.967 units. The energy of a chain with an equidistant distribution of the PDs is 11.974 units. The structure has the PDs $\phi_i = (i - 1) 2\pi/N$ giving $(0, 0.63, 1.26, 1.89, 2.51, 3.15, 3.77, 4.4, 5.03, 5.66)$. An equally distributed chain, Φ , of length 2π needs a nearly equal amount of force to move along the site-up potential. Thus the PES profile line can really flatten out. One could guess that this is the end of the story? (Compare the pre-structure in Fig. 13.) But a further, strong excitation with $F_{dc}=25$ makes a ‘line’ at the energy of 11.975, over the equidistant distribution of the PDs. The chain itself is here a little bit compressed, on its way ‘downhill’ the sliding. Its length varies between 5.63 and 5.68 being smaller than 2π .

On the other hand, the example of an excitation with $F_{dc} = 25$ is far over the symmetric SP_3 of the case $M = 0$ lying at 20 units of energy. If one assumes here an inverse ‘relaxation’ of the not fully stretched chain from the $M = 1$ to the $M = 0$ case, one would get a

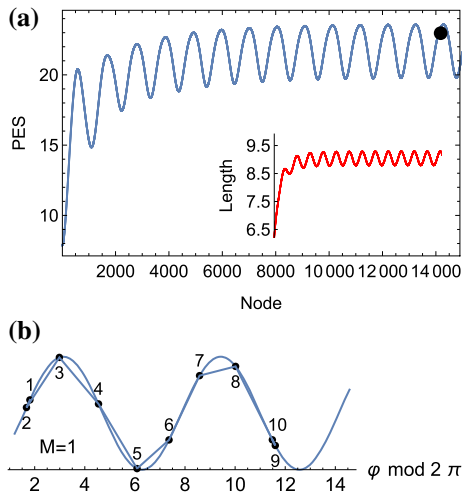


Fig. 15 a Langevin profile (PES only) for a non unique excitation, see text. The red inlay is the changing of the length of the chain under the ‘downhill’ sliding with this force. The black bullet in the upper right corner is a possible entry point to a ‘wormhole’ to $M = 2$. Its structure is given in panel b

back jump and the pure whirling of the chain as a lump, like in Sect. 3.

All in all, we cannot see a resonant oscillation of the chain at the fin of the ZFS [6]. In contrast we detect no kind of vibration, but only a straight, stiff ‘downhill’ sliding of the chain.

Conjunction

The reason for the ZFS is that the force for the movement of the chain can increase, but the PES flank becomes steeper, to vertical. So the increase of the level line goes to zero. The relation of the PDs to the voltage of experiments is given by the Josephson voltage-phase equation [12, 47]

$$V_j = \frac{\Phi_0}{2\pi} \langle \dot{\phi}_i \rangle \tag{11}$$

where $\langle .. \rangle$ means time average. If the ϕ_i all move with equal distance and velocity, we get a constant voltage. Note that the relation (11) can be directly transformed into the usual current-voltage characteristics.

We imagine the different cases of the external excitation, \mathbf{f} , in Fig. 12 with the help of Fig. 3. The chain is uniformly driven by the ‘washboard’ force to all directions $\mathbf{f} = F/\sqrt{10}(1, \dots, 1)^T$. However, it is moved by the component f_k only over the k -th SP₁ where the PD ϕ_k is on top of the cosine function. The other components act in the moment to other dimensions. Thus, the driving is, so to say, inefficient. The orthogonal components to the MEP of \mathbf{f} are consumed with unnecessary energy. This explains why the solutions of the Langevin equation do not follow the MEP but are moved somewhat uphill on the flank of the PES. However, the Langevin solution goes somewhat parallel to the MEP.

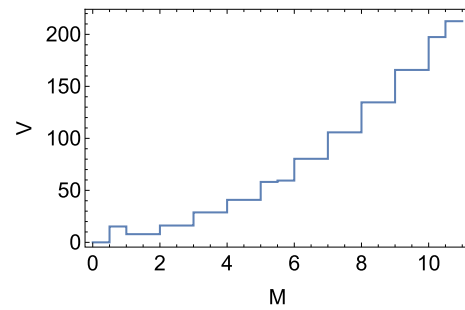


Fig. 16 Ladder of energy levels of the MEP for different numbers of fluxons, M . Note that steps for $M > N/2$ are not realized in experiments, by symmetry reasons [9, 12, 24] caused mainly by the PBC (3)

Table 1 MEP levels to different fluxons

M	0	1	2	3	4	5
$V(\Phi_{\min})$	0	7.87	16.17	28.8	40.85	58.12

We study the character of the point on the PES for the equidistant distribution of the PDs, compare Fig. 14. The gradient there does not have equal components but is symmetric: $(0, 0.588, 0.951, 0.951, 0.588, 0, -0.588, -0.951, -0.951, -0.588)$, and it is of course not near the zero vector, and the determinant of the Hessian is negative. An eigenvector to the one negative eigenvalue is $(0.02, 0.035, 0.101, 0.257, 0.486, 0.61, 0.486, 0.257, 0.101, 0.035)$ which is orthogonal to the gradient.

In Fig. 14 the 2D projected PES at the equidistant structure of the chain is shown. It seems that the point of interest could be near a valley-ridge inflection (VRI) point of a ridge of the 10D PES. An NT to the downhill direction correctly gives a known minimum. It seems that Fig. 14 represents a piece of Fig. 3. An NT going uphill this structure starts the folding of the chain, but we could not find any ‘folded’ SP. Diverse NTs going uphill turn back later after passing only TPs.

4.4 A possible ‘wormhole’ for a jump to $M = 2$, once more Middleton’s no-passing rule

The last subsection has demonstrated that an external excitation of the ring chain by a totally symmetric force vector, $(1, 1, \dots, 1)$, climbs up the wall quasi parallel to the floor of the MEP, compare Fig. 3. But because the wall becomes steeper and steeper, the increase of energy height, thus the increase of the ‘speed’ of the chain on its ‘downhill’ sliding on the effective PES will become smaller and smaller. We guess that this is the reason for the measured ZFS in experiments.

How can a jump to the next M state happen, or with the experimental result, how can the array switch to a higher voltage state [10]? We assume that the excitation of the chain is not totally symmetric. In an experiment one can imagine, besides the omnipresent noise [48], that one can change the array parameters [17] by

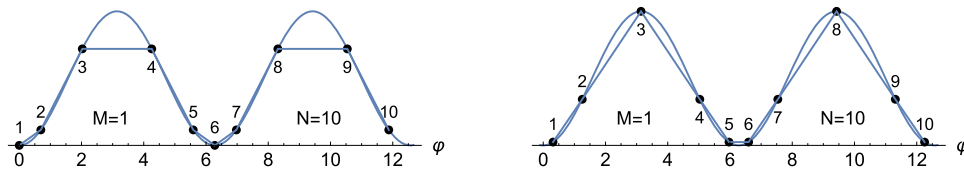


Fig. 17 Extended two fluxons of the chain for PBC $M = 2$ with the minimum (left) and SP_1 (right). The SP_1 is symmetric, but the ϕ_1 disturbs the symmetry for the minimum

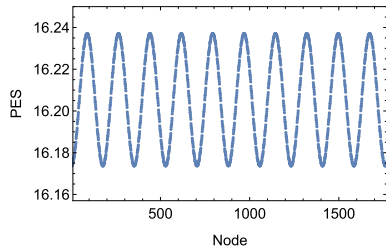


Fig. 18 Energy profile over the MEP through minimums and SP_1 of Fig. 17 calculated by an NT to unitary direction $(1, \dots, 1)$. Note again the very low energy difference of the two stationary points. Thus, the pathway again is nearly flat

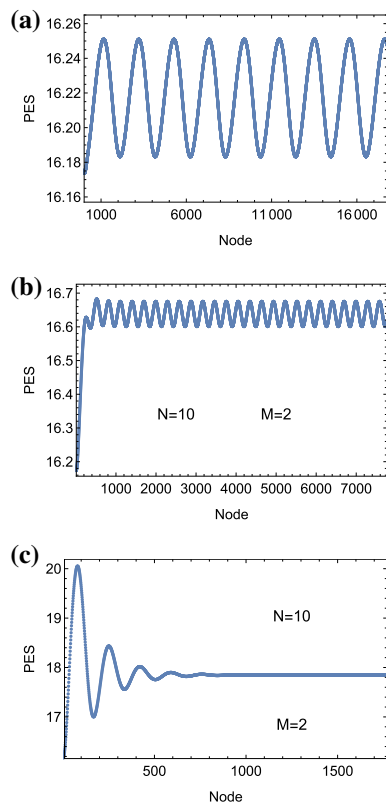


Fig. 19 Energy profile of three dc-driven Langevin solutions in case $M = 2$ on the PES only (without representation of the tilting) for $N = 10$ PDs. **a** For $F_{dc} = 0.15$ with the start in a minimum, **b** for $F_{dc} = 1$, and **c** for $F_{dc} = 7.5$. We find a stable small vibration in cases **a** and **b** after an initial settling. In case **c** the curve flattens out quite analogously to the case $M = 1$. Note the different t -scales in the three panels

the plaquette self-inductance, or by the single JJ critical currents. Additionally, in some experiments [12] the current is actually injected at one JJ, instead of all JJs. So, we take for a calculation an unsymmetrical excitation direction

$I_{wormhole} = 1/3.26$ (0.5, 0.75, 1, 1, 1, 1, 1, 1.25, 1.5) with norm 1, and the large amount $F_{dc} = 20$.

Figure 15a shows the profile of the Langevin solution, being somewhat similar to former curves. The red inlay is the length of the chain: it becomes stretched because of the unsymmetrical force. The black bullet is a structure, shown in panel (b) which has 3 PDs in the left well, 4 PDs in the central well, but 3 PDs in the right well of the cosine function. This structure will relax to the SP_1 , or to the minimum of the case $M = 2$, (see Sect. 4.3 below) if the ring condition of the PBC is put to $M = 2$. The chain can jump to the next M like this. Because the ‘floors’ of the PES to different M values have different energies (see Fig. 16 and Table 1 below) we get for the transitions between the branches in the experiments a discontinuous voltage [47].

Note again an interchange of ϕ_1 and ϕ_2 , as well as of ϕ_9 and ϕ_{10} , of the ‘wormhole’-entry. Thus the no-passing rule here is injured as well. Though, in this case, the force vector has only positive components, in contrast to Sect. 4.2. The reason for the interchange of the outer PDs may be the strong action of the PBC (5). One may see this structure as a beginning of a folding, like the SP_1 of the $M = 0$ -case.

Note that the exact calculation seems quite difficult, for which high F_{dc} amount, for which slightly unsymmetrical force, and at which point on the pathway of the chain ‘downhill’ such an entry point first emerges. Our example only demonstrates the existence of such a point. One hint can give the minimal energy step which one should apply to jump from the minimal floor of one M to the next floor for $M + 1$, which is represented in the scheme of Fig. 16, compare Sect. 5 for the cases $M = 3$ to 10.

4.5 The movement of an FK chain for $M = 2$

Two ‘fluxons’ of the PDs can emerge in the ring, see Fig. 17 for the structure of a minimum and an SP_1 . Their energies are 16.173 and 16.237 units, correspondingly. An NT which connects consecutively the minimums and the SP_1 with a wandering top ϕ_i is given in Fig. 18. It is similar to former cases in Figs. 2 and 6(a).

In Fig. 19 we show calculations of a ‘sliding chain’, a solution of the Langevin Eq. (10), which quickly finds

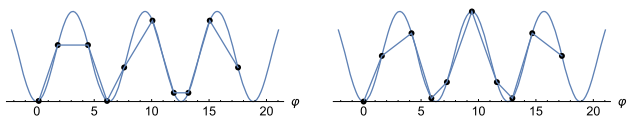


Fig. 20 Minimum left and SP_1 right of the FK chain with $N = 10$ PDs under the ring condition (5) with $M = 3$ fluxons. There exists a mirror symmetric structure of the minimum (not shown)

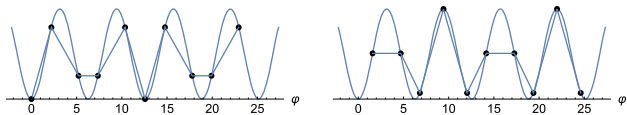


Fig. 21 Minimum left and SP_1 right of the FK chain with $M = 4$ fluxons

the region over the MEP and then goes on up to infinity. Note that the pathway of the MEP is (for $k = 1$ and $M=2$ also) quasi flat. The profiles follow again the pattern of the MEP between the minimum and the SP_1 of the chain in Fig. 18, on an increasing level of energy.

In panel Fig. 19a we find, after a short settling, that the flow oscillates by a fixed, but low frequency. The profile repeats the MEP of Fig. 18 however, on a higher energy level. The minima and maxima of the profile are TPs but not stationary points of the PES.

To (b): after less than 500 t -steps (nodes) the chain slides ‘down’ the tilted effective PES by a stable flow with a much higher frequency than in case (a). However, the amount of the vibration decreases. The projected profile on the original PES is much higher than the MEP.

To (c): a giant settling takes place for the large F_{dc} . But after less than 1000 t -steps the vibration flattens out and ‘stays’ without a vibration at 17.847 units.

5 Structures of the FK chain for $M = 3$ to $M = 10$

The stationary structures of the chain for $M = 3$ are shown in Fig. 20. The MEP for $M = 3$ is similar to former cases, compare Figs. 2 and 18. Energies are 26.805 units for the minimum and 26.81 for the SP_1 , so the MEP between the stationary points becomes very flat. Langevin solutions exist for the depinned chain sliding ‘downwards’ similarly to Fig. 19.

The stationary structures of the chain for $M = 4$ are shown in Fig. 21. The MEP for $M = 4$ is similar to former cases, see Figs. 2 and 18. Energies are 40.852 units for the minimum and 40.885 for the SP_1 . Langevin solutions exist for the depinned chain sliding ‘downwards’ similarly to Fig. 19.

The stationary structures of the chain for $M = 5$ are shown in Fig. 22. Although 5 PDs are on the tops of the site-up potential at the SP, it has indeed index one. The character of the PES changes if the boundary conditions are removed (but $a_0 = \pi$ is used). Then

the same SP structure has the SP index 2. Besides the given SP structure exits a mirror symmetrical SP. The MEP for $M = 5$ is similar to former cases in Figs. 2 and 18. Energies are 58.123 units for the minima and 59.348 for the SP_1 . The left minimum goes over 5 wells with a length of 27.789, but the right minimum is longer and extends over 5 hills with a length of 28.76. The two SPs have the exact length of $9\pi=28.274$ being in between. The example again demonstrates that the average distance of the chain, \tilde{a}_0 , is not constant at $2\pi M/N$ [24]. The PBC goes into the potential energy ansatz (5) as a part of the potential energy. It is $\tilde{a}_0 \approx 2\pi M/N$ only approximately realized. The reason is that the PBC demands that $\phi_{N+1} - \phi_1 = 2\pi M$, however, the distance $\phi_{N+1} - \phi_N$ is variable for the forces of the FK model, as well as all other distances of the chain.

For an $M = N/2$ case an experiment notes a small depinning current [9]. It corresponds to the larger difference of the two energies of 1.225 units in this case, the Peierls-Nabarro barrier [49], being higher in comparison to the cases of former $M > 0$. Langevin solutions exist for the depinned chain sliding ‘downwards’, see the right pannel in Fig. 22. The force amount F_{dc} must be higher than the critical force at the barrier breakdown point (BBP) [2] of the PES. If the 5 fluxon chain moves along the MEP then it has to alternate from the ‘long’ minimum to the ‘right’ SP (where the 5 top PDs are at the right-hand side), to the ‘short’ minimum, and then to the ‘left’ SP, and so on. It is clear that this process does not take place by a rigid chain, a ‘rigid fluxon’ [27] which is claimed to represent a quasiparticle. No, the chain always changes its length. It is not rigid.

The case of $M = N/2$ has already been discussed in part I [1] for an additional ac -excitation of the chain. Then Shapiro steps emerge.

We add Table 1 with the minimum energies on the MEP to different fluxon numbers, M . These energies are not linear in M . It is claimed that in an experiment the M fluxons are set by a magnetic field of ‘about M flux quanta Φ_0 corresponding to exactly M vortices of the ring’ [9]. This cannot be exactly correct in view on the nonlinear dependence of the energies of the floors on the number M , see Table 1.

In contrast, workers in Ref. [50] write that they could not experimentally determine the exact number of fluxons in the ring. So, there is no universal agreement among different experiments.

The stationary structures of the chain for $M = 6$ are shown in Fig. 23. The MEP for $M = 6$ is similar to former cases, see Figs. 2 and 18. Energies are 80.33 units for the minimum and 80.363 for the SP_1 . The structures are a kind of mirror picture to the $M = 4$ -case. It is known that due to symmetry the average distance \tilde{a}_0 can be restricted to the interval $[0, \pi]$ without loss of generality [24]. One has to contract here all ϕ_i by the factor $4/6$. We get a formula for the single PDs (by N even) with

$$\phi_j \Big|_{\frac{N}{2}-k} \left(\frac{N}{2} + k \right) = \phi_j \Big|_{\frac{N}{2}+k} \left(\frac{N}{2} - k \right) \quad (12)$$

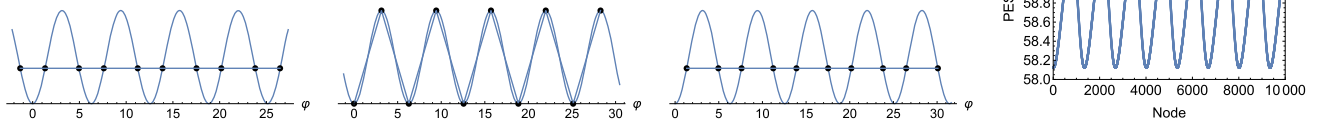


Fig. 22 Minimum left, SP_1 centre left, and second minimum centre right, of the FK chain with $M=5$ fluxons. Both minimums have the same energy, but a different length. There exists a mirror symmetric SP (not shown). The right panel is the energy profile over the MEP through minimums and SP_1 calculated by a Langevin equation with unitary direction $(1, \dots, 1)$

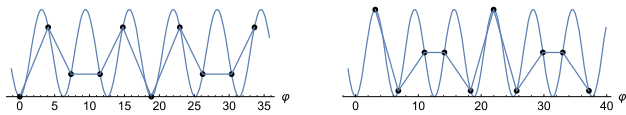


Fig. 23 Artificial minimum left and SP_1 right of the FK chain with $M = 6$ fluxons

for $j = 1, \dots, N$, $1 \leq k < \frac{N}{2}$. On the left hand side we have real structures of the chain, but on the right hand side we find only artificial structures. For $M = 6$ distances between the PDs are much more stretched, thus the energy levels would be much higher. Equivalently to the symmetry treatment [12], in experiments [9, 50] is reported that the steps with $M = N/2 + k$ give equal I/V curves like the steps with $M = N/2 - k$ for $k = 1, \dots, N/2 - 1$. Thus these steps with $M > N/2$ do not emerge, at all. The much higher energy of the ‘overstretched’ structures is not realized. The spring formulas (4) and (5) allow for $M > N/2$ an artificially overstretched solution. Nature, however, does not realise this solution.

Energies for $M = 7$ are 105.762 units for the artificial minimum and 105.766 for the artificial SP_1 . Again the structures are a mirror picture to the $M = 3$ -case. One has to contract all ϕ_i by the factor $3/7$. Equation (12) here also applies.

Energies for $M = 8$ are 134.609 units for the artificial minimum and 134.672 for the artificial SP_1 . The structures are a mirror picture to the $M = 2$ -case. One has to contract all ϕ_i by the factor $2/8$. Equation (12) here also applies.

Energies for $M = 9$ are 165.782 units for the artificial minimum and 165.808 for the artificial SP_1 . And the structures are a mirror picture to the $M = 1$ -case. One has to contract all ϕ_i by the factor $1/9$. Equation (12) here also applies.

The artificial stationary structures of the chain for $M = 10$ are shown in Fig. 24. Energies are 197.392 units for the minimum, 212.648 for the SP_1 , 212.686 for the SP_2 , and 217.392 for the SP_3 . The difference of SP_3 to the minimum is 20 units like in the case $M = 0$. A comparison with the folded structures of the SP_1 and SP_2 of the $M = 0$ -case shows that here the structures are unfolded, like in the other cases for $0 < M < 10$. However, the unnecessary ‘overstretched’ structures are not realized in experiments, there is an energy penalty. For the minimum, one can see the ‘impossibility’ because

all $\phi_i \equiv 0 \pmod{2\pi}$. The case $M = N$ (winding number $\omega = 1$) which is discussed in reference [44], is an abstraction which has no realisation for the PBC (3). It is a mathematical extension to play with.

6 Impurities

We have seen in Sect. 4 that some ‘theoretical’ problems emerge if we deal with the symmetric array of JJs under a fully symmetric excitation. The pathway of the chain of PDs will then hold the symmetry, being usually a way on a ridge on the PES, but it does not find the quite lower, unsymmetric region of the corresponding MEP. However, if the chain is disturbed, from the early beginning, by any kind of impurity then the symmetry-‘problem’ come off by itself.

7 The folding problem

If ϕ_1 and ϕ_N have the ‘correct’ distance of the PBC, $\approx 2\pi M(N-1)/N$, then nevertheless other ϕ_i can be in a ‘false’ order. Thus the distances $\Delta\phi_i$ can have positive or negative values. Compare the folded SP_1 and SP_2 of case $M = 0$ in Sect. 4.1. The possibility emerges in calculations of the entry of the ‘wormhole’ in Sect. 4.4, or of NTs in higher energy regions of the PES because the ‘ordering’ action of an $a_0 > 0$ is missing in the model.

An example is a VRI point with an energy of 21.96 units for $M = 1$. The PDs are (1.46, 3.65, 4.79, 4.56, 3.14, 1.73, 1.5, 2.63, 4.82, 6.28) modulo 2π . ϕ_1 to ϕ_4 are ordered correctly, but ϕ_5 to ϕ_7 go backwards, and at the end ϕ_8 to ϕ_{10} are again ordered correctly. The structure is two times folded.

However, we did not find any SP with such a folded structure for $M > 0$.

8 Discussion

An interesting question for the imagination is: how one has to imagine the tilting of the annular chain by the washboard potential, thus by the unitary external

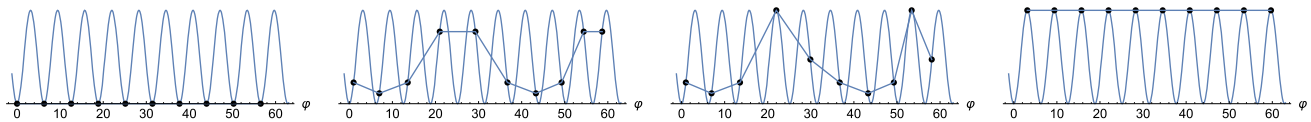


Fig. 24 Artificial equilibrium structures of the FK chain with $M = 10$ fluxons. Left to right: minimum, SP_1 , SP_2 , and SP_3

force? So to say, the externally excited JJs array is a real example for M. C. Eschers ‘waterfall’ [51]. The explanation is the ‘topological constraint’ of Eq. (3) [12] enforcing a cycle. “In a cyclic process, the arrow of time is made circular” [52].

In all cases of $M > 0$ we have to realise that the PBC (5) is a strong force in our potential formula. It dictates the shape of the FK chain, compare the structure Figs. 1, 4, 16, and 20, 21, 22, 23 and 24. In all cases $0 < M < 10$ we have one deep valley with the MEP over the minimums and the SP_1 on nearly the same level. The MEP crosses all N dimensions and closes to the ring by the PBC. There is only this one floor, and nothing else. The remaining PES has only steep flanks tending to vertical walls. It seems that no further SPs exist, at least not in a usefull energy region. So to say, we find a very simple PES, in contrast to part II [2]. Of course, different floors emerge for different numbers of fluxons, M .

We can explain the ZFS by the use of a Langevin equation only, for $0 < M \leq N/2$. It is a simplification but it is sufficient. We do not need the full, more correct equations of motion with the second derivatives. Thus, we do not treat the radiation of small amplitude waves (phonons) of the chain [11, 12, 18, 53]. The PES (6) is the same for both equations, of first or second order. Possibly, a further internal vibration of the chain could make the entry into a ‘wormhole’ for the transition from a given floor of M fluxons to the floor of $M + 1$ ones easier. The question deserves further study, compare Ref. [11] which, on the other hand, uses a very larger $N = 50$ and a very smaller k -parameter between 0.5 and 0.25.

The deep minimum well of the PES in case $M=0$ makes it possible that the chain vibrates along with the N different normal modes. However, in the cases $M > 0$ we do not find a deep minimum well. The MEP is a very flat ‘floor’ on the PES for spring parameter $k = 1$. For $M=1$ we have the lowest eigenvalue of the Hessian at the minimum at 0.06 units, and the decay direction of the SP_1 has the eigenvalue -0.058 . The barrier is 0.025 units. Here cannot exist a vibration of the chain with a frequency such that it can be fitted more or less along this MEP. Here does not exist a ‘kink internal mode’ [54] along the MEP. (One can imagine vibrations orthogonal to the MEP. They can be named breathers [47] indicated by a single $l_i = 1$, but all other $l_{j \neq i} = 0$. However, these we do not need for a sliding. They make the treatment only more complicated.) A low external force with $F/\sqrt{10} > F_c$, the critical force, induces a depinning and avoids any vibration. The sliding of the chain is indeed a rotation through the JJs array, by the

PBC. And this rotation will have a ‘frequency’ determined by the velocity of the chain. Note that we never observed a whirling of parts of the chain [41].

In the FK model with free boundaries [2] kinks and antikinks have an own length which is determined by the parameters of the model, ($v = 1$ here) and k , the ratio of the parts of the potential energy. Under the PBC (5) the chain is, for $M > 0$, stretched over the full interval, $2\pi M$. This means that the corresponding fluxon does not have an own length. The chain itself is the fluxon. The observation is in contrast to ref. [21] which claims that the $2\pi M(N-1)/N$ form is too crude to grasp the crucial points of the problem, and demands that the kink is not an $\approx 2\pi M$ form. We must determine here that the ansatz (5) acts in our description; the mathematics is not negotiable.

We guess that there are not such constructs like anti-fluxons which can annihilate themselves with fluxons [6, 8]. We guess that there cannot be more than one single fluxon in the chain with a different velocity [10]. We guess that there cannot be an addition of, for example, two fluxons with $1M$, to one fluxon with $2M$ [10, 18]. At least not in this FK model with the PBC. The reason is that for every M only one minimum exists, and only one SP_1 structure (besides the numbering of the PDs, and their ‘rotation’). Different fluxon structures for a fixed M are not compatible with such a simple PES, at least not for our small $N = 10$.

In all parts of this series, I, II, and this paper, compare refs. [1, 2], we start with an FK model by its mathematical formula, including the corresponding boundary condition. Using corresponding properties of the models, we demonstrate how the models allow diverse stationary states, or flows of the chain of particles, or parts like the phase differences ϕ_i in this paper. We claim that this simple mathematical analysis, as we did it, is essential for the decision that the FK formulae can be a model for the explanation of diverse experiments.

So far the treatment of resonant steps in FK models has mainly be restricted to describe ‘that they emerge’, but not yet extended to explain ‘why they emerge as they are’. This we try in the series of the three papers. The main tool is the study, the development of the old known PES of the current model, its global and intermediate minimums, and its SPs of an increasing index, and of possible low energy paths connecting diverse stationary points. We resolve that these paths and their neighbourhoods on the PES are often the sliding regions of the chain under the external force, which (we guess so) are also implicitly used by older simulations of the sliding of FK chains by other groups.

9 Conclusion

By analysing the PES of the FK model with PBC we can describe the stationary states forming the pathway for a sliding of the chain. Which in reality is a rotation of one or more fluxons through the annular JJs. For increasing external forces we get an explanation for the zero-field steps (ZFS) by nearly vertical walls of the PES. We can assign the different number of fluxons, M , to different structures of the chain. We propose a mechanism for the jump of the chain from M to $M + 1$. The first such jump from $M = 0$ happens at an SP of index one quite exactly at the corresponding critical force to overcome this SP, where a folded chain structure relaxes to the $M = 1$ minimum. However, for higher M one has to stretch the chain up to a length where it can relax to the next $M + 1$. But note that we need an unsymmetrical force for the explanation, in both cases.

Author contributions

All authors contributed equally to the paper.

Funding Open Access funding enabled and organized by Projekt DEAL. We acknowledge the financial support from the Spanish Ministerio de Economía y Competitividad, Projects No.PID2019-109518GB-I00, Spanish Structures of Excellence Mariá de Maeztu program through grant MDM-2017-0767 and Generalitat de Catalunya, project no. 2017 SGR 348.

Availability of data Data of all stationary states reported in the paper are available on request by WQ.

Declarations

Conflicts of interest There is no conflict of interest.

Open Access This article is licensed under a Creative Commons Attribution 4.0 International License, which permits use, sharing, adaptation, distribution and reproduction in any medium or format, as long as you give appropriate credit to the original author(s) and the source, provide a link to the Creative Commons licence, and indicate if changes were made. The images or other third party material in this article are included in the article's Creative Commons licence, unless indicated otherwise in a credit line to the material. If material is not included in the article's Creative Commons licence and your intended use is not permitted by statutory regulation or exceeds the permitted use, you will need to obtain permission directly from the copyright holder. To view a copy of this licence, visit <http://creativecommons.org/licenses/by/4.0/>.

References

1. W. Quapp, J.M. Bofill, Eur. Phys. J. B **94**, 66 (2021). (Part I of this series)
2. W. Quapp, J.M. Bofill, Eur. Phys. J. B **94**, 64 (2021). (Part II of this series)
3. T.A. Fulton, R.C. Dynes, Solid State Comm. **12**, 57 (1973)
4. B.D. Josephson, Phys. Lett. **1**, 251 (1962)
5. S. Shapiro, Phys. Rev. Lett. **11**, 80 (1963)
6. J.J. Mazo, A.V. Ustinov, The sine-Gordon Equation in Josephson-Junction Arrays (Springer International Publishing, Switzerland, 2014), chap. 10, pp. 155–175
7. I.R. Rahmonov, J. Tekić, P. Mali, A. Irie, Y.M. Shukrinov, Phys. Rev. B **101**, 024512 (2020)
8. A. Davidson, B. Dueholm, B. Kryger, N.F. Pedersen, Phys. Rev. Lett. **55**, 2059 (1985)
9. H.S.J. van der Zant, T.P. Orlando, S. Watanabe, S.H. Strogatz, Phys. Rev. Lett. **74**, 174 (1995)
10. J. Pfeiffer, M. Schuster, A.A. Abdumalikov Jr., A.V. Ustinov, Phys. Rev. Lett. **96**, 034103 (2006)
11. J. Pfeiffer, A.A. Abdumalikov Jr., M. Schuster, A.V. Ustinov, Phys. Rev. B **77**, 024511 (2008)
12. S. Watanabe, H.S.J. van der Zant, S.H. Strogatz, T.P. Orlando, Phys. D **97**, 429 (1996)
13. W. Quapp, J.M. Bofill, Mol. Phys. **117**, 1541 (2019)
14. W. Quapp, J.M. Bofill, Eur. Phys. J. B **92**, 95 (2019)
15. W. Quapp, J.M. Bofill, Eur. Phys. J. B **92**, 193 (2019)
16. W. Quapp, J.Y. Lin, J.M. Bofill, Eur. Phys. J. B **93**, 227 (2020)
17. F. Faló, P.J. Martínez, J.J. Mazo, T.P. Orlando, K. Segall, E. Trías, Appl. Phys. A **75**, 263 (2002)
18. A.V. Ustinov, M. Cirillo, B.A. Malomed, Phys. Rev. B **47**, 8357 (1993)
19. P. Caputo, A.V. Ustinov, N. Iosad, H. Kohlstedt, J. Low Temp. Phys. **106**, 353 (1997)
20. J.J. Mazo, F. Narajo, K. Segall, Phys. Rev. B **78**, 174510 (2008)
21. Z. Zheng, B. Hu, G. Hu, Phys. Rev. B **58**, 5453 (1998)
22. G. Kathriel, SIAM J. Math. Anal. **36**, 1434 (2005)
23. G. Chu, J.V. José, Phys. Rev. B **47**, 8365 (1993)
24. T. Strunz, F.J. Elmer, Phys. Rev. E **58**, 1601 (1998)
25. A. Saadatpour, M. Levi, Phys. D **244**, 68 (2013)
26. F. Naranjo, K. Segall, J.J. Mazo, Eur. Phys. J. B **88**, 185 (2015)
27. J. Tekić, Personal communication (2020)
28. C. Baesens, R.S. MacKay, Nonlinearity **11**, 949 (1998)
29. O.M. Braun, A.R. Bishop, J. Röder, Phys. Rev. Lett. **79**, 3692 (1997)
30. O.M. Braun, Y.S. Kivshar, Phys. Rep. **306**, 1 (1998)
31. A.B. Koltun, D. Domínguez, N. Grønbech-Jensen, Phys. Rev. Lett. **86**, 4112 (2001)
32. J. Tekić, P. Mali, The Ac Driven Frenkel-Kontorova Model (University of Novi Sad, Novi Sad, 2015)
33. O. Braun, T. Dauxois, M. Paliy, M. Peyrard, B. Hu, Phys. D **123**, 357 (1998)
34. Y.P. Monarkha, K. Kono, Low Temp. Phys. **35**, 356 (2009)
35. W. Quapp, J.M. Bofill, Theoret. Chem. Acc. **135**, 113 (2016)
36. W. Quapp, J.M. Bofill, J. Ribas-Ariño, Int. J. Quant. Chem. **118**, e25775 (2018)
37. J.M. Bofill, J. Ribas-Ariño, S.P. García, W. Quapp, J. Chem. Phys. **147**, 152710 (2017)
38. W. Quapp, J.M. Bofill, Int. J. Quant. Chem. **118**, e25522 (2018)

39. J.M. Bofill, R. Valero, J. Ribas-Ariño, W. Quapp, J. Chem. Theo. Comp. **17**, 996 (2021)
40. M. Levi, Dynamics of Discrete Frenkel-Kontorova Models, in: Analysis, Et Cetera, Eds.: P. H. Rabinowitz, E. Zehnder, (Academic Press, Cambridge, 1990), pp. 471–494
41. S. Watanabe, S.H. Strogatz, H.S.J. van der Zant, T.P. Orlando, Phys. Rev. Lett. **74**, 379 (1995)
42. A.V. Ustinov, Phys. D **123**, 315 (1998)
43. S. Gombar, P. Mali, S. Radošević, J. Tekić, M. Pantić, M. Pavkov-Hrvojevic, Phys. Scr. **96**, 035211 (2021)
44. J. Tekić, A.E. Botha, P. Mali, Y.M. Shukrinov, Phys. Rev. E **99**, 022206 (2019)
45. A.A. Middleton, D.S. Fisher, Phys. Rev. B **47**, 3530 (1993)
46. P.S. Lomdahl, O.H. Soerensen, P.L. Christiansen, Phys. Rev. B **25**, 5737 (1982)
47. P. Binder, D. Abraimov, A.V. Ustinov, S. Flach, Y. Zolotaryuk, Phys. Rev. Lett. **84**, 745 (2000)
48. J. Theiler, S. Nichols, K. Wiesenfeld, Phys. D **80**, 206 (1995)
49. Y.S. Kivshar, D.K. Campbell, Phys. Rev. E **48**, 88 (1983)
50. K. Segall, A.P. Dioguardi, N. Fernandes, J.J. Mazo, J. Low Temp. Phys. **154**, 41 (2009)
51. M.C. Escher, *Waterfall - Lithograph* (1961)
52. A. Valizadeh, M.R. Kolahchi, J.P. Straley, J. Nonlin. Math. Phys. **15**, 407 (2008)
53. M. Peyrard, M.D. Kruskal, Phys. D **14**, 88 (1984)
54. O.M. Braun, Y.S. Kivshar, M. Peyrard, Phys. Rev. E **56**, 6050 (1997)